

Charge Excitation Dynamics in Bosonic Fractional Chern Insulators

Xiao-Yu Dong,¹ Adolfo G. Grushin,^{2,3} Johannes Motruk,^{2,4} and Frank Pollmann^{1,5}

¹Max-Planck-Institut für Physik komplexer Systeme, Nöthnitzer Straße 38, 01187 Dresden, Germany

²Department of Physics, University of California, Berkeley, California 94720, USA

³Institut Néel, CNRS and Université Grenoble Alpes, Grenoble, France

⁴Materials Science Division, Lawrence Berkeley National Laboratory, Berkeley, California 94720, USA

⁵Technische Universität München, Physics Department T42, 85747 Garching, Germany

 (Received 1 November 2017; revised manuscript received 6 April 2018; published 20 August 2018)

The experimental realization of the Harper-Hofstadter model in ultracold atomic gases has placed fractional states of matter in these systems within reach—a fractional Chern insulator state (FCI) is expected to emerge for sufficiently strong interactions when half-filling the lowest band. The experimental setups naturally allow us to probe the dynamics of this topological state; yet little is known about its out-of-equilibrium properties. We explore, using density matrix renormalization group simulations, the response of the FCI state to spatially localized perturbations. After confirming the static properties of the phase we show that the characteristic, gapless features are clearly visible in the edge dynamics. We find that a local edge perturbation in this model propagates chirally independent of the perturbation strength. This contrasts the behavior of single particle models with counterpropagating edge states, such as the noninteracting Harper-Hofstadter model, where the chirality is manifest only for weak perturbations. Additionally, our simulations show that there is inevitable density leakage from the first row of sites into the bulk, preventing a naive chiral Luttinger theory interpretation of the dynamics.

DOI: [10.1103/PhysRevLett.121.086401](https://doi.org/10.1103/PhysRevLett.121.086401)

Introduction.—Understanding the dynamical properties of strongly correlated quantum phases in dimensions higher than one still remains a difficult challenge in the vast majority of cases [1,2]. The lack of a complete paradigm originates from the inherent complexity of simulating the dynamics of strongly interacting quantum systems. However, modern experiments [3–7] are now able to access time-dependent properties and thus the need to precisely characterize dynamical signatures of correlated phases is becoming pressing. Among the most intriguing are scenarios in which topology joins in as an additional ingredient of the system.

A recent prominent example is the realization of the Chern insulator phase using ultracold atoms, both in a bosonic Harper-Hofstadter model [8–11] and the fermionic Haldane honeycomb model [12,13]. In both cases, periodically driving a lattice loaded with ultracold atoms has been proven to show topological features [13,53], as predicted by general theoretical arguments based on Floquet theory [14–18]. On-site interactions in the Harper-Hofstadter realization can drive the system into a bosonic Floquet fractional Chern insulator (FCI) state [19–28], the bosonic periodically driven analog of the fractional quantum Hall (FQH) effect [29–34]. Several protocols have been proposed to prepare this state and the phase diagram of the Harper-Hofstadter model for hardcore bosons has been established using various numerical methods [31,33,35]. Although this body of knowledge

combined with proposals to detect chiral edge states [36–38] hinted at how to identify the existence of the FCI state in cold atomic experiments, simulations of dynamical signatures of this phase are still lacking. However, the observation of time-dependent quantities in this system is possible, due to the high tunability of parameters and slow dynamics compared to the solid state, and necessary, due to the difficulty of probing transport quantities characterizing these states, such as the Hall conductivity.

In this Letter we address dynamical properties of the edge of the FCI phase of hardcore bosons at filling factor $\nu = 1/2$ after local quenches using matrix-product state (MPS) based simulations. We use the density matrix renormalization group (DMRG) method together with a recently introduced method [50] that allows for the efficient simulation of the dynamical response function in two-dimensional systems [51]. Our goal is to provide distinct dynamical signatures of the FCI phase which could be probed with current state of the art experiments. By adding a particle at the edge we find a clear chiral propagation of the FCI gapless edge modes, characteristic for such phases (see Fig. 1). Moreover, this protocol provides a simple distinction between an emergent Laughlin state and a noninteracting Chern insulator (CI) that hosts multiple edge modes of opposite chirality. The latter shows no chiral asymmetry, while the chirality in the former case is clearly visible. The reason is that a generic perturbation in the noninteracting case mixes edge states with opposite

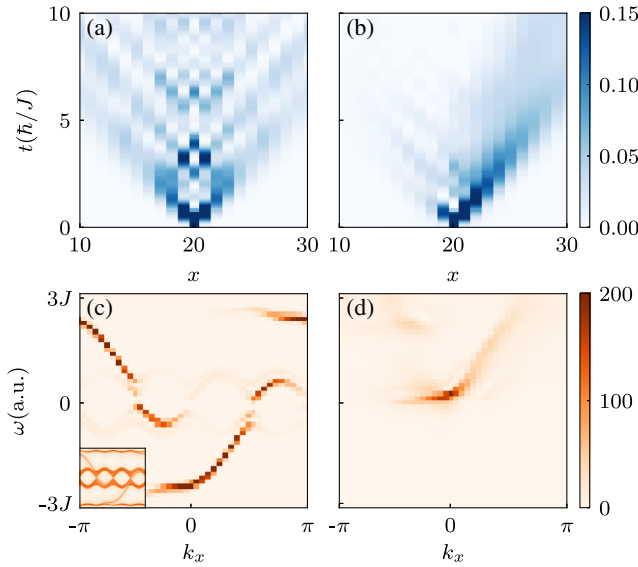


FIG. 1. Time evolution of the particle density in the Harper-Hofstadter model after a particle has been created at the edge of an empty vacuum state with total filling $\nu = 0$ (a) and in the interacting FCI state at $\nu = 1/2$ of the lowest band (b). The spectral function $A(k_x, \omega)$ of the noninteracting case (c) reveals a prominent overlap with gapless edges states of both chiralities. The inset shows for comparison the density of states of the single-particle model. In contrast, the spectral function for the FCI (d) shows a single chiral mode.

chirality while the chirality in the Laughlin case is protected by the many-body bulk state. As an experimentally relevant example we study the $\phi = \pi/2$ Harper-Hofstadter model at total filling $1/8$ [8–11] and propose a protocol that applies a local trap at the edge to distinguish the FCI state by varying the trap strength.

Static properties.—We consider the Harper-Hofstadter Hamiltonian [8,9],

$$H = -J \sum_{\langle ij \rangle} (e^{i\phi_{ij}} a_i^\dagger a_j + \text{H.c.}), \quad (1)$$

on a square lattice with a magnetic flux of $\phi = \pi/2$ per plaquette. Here a_i^\dagger (a_i) creates (annihilates) a hardcore boson on site i . The single-particle spectrum of H has four bands [see Fig. 1(c), inset] with the central bands touching at four Dirac points. The model is characterized, from top to bottom, by three Chern numbers $C_i = \pm(1, -2, 1)$, where the sign is determined by the sign of ϕ . We start by verifying that H indeed hosts a $\nu = 1/2$ Laughlin state in agreement with previous results [29–33,39]. For this we simulate Hamiltonian (1) on an infinite cylinder of circumference L_y and total filling $1/8$ with DMRG, which enforces the half-filling of the lowest Chern band. The results are summarized in Fig. 2 and Ref. [40], which confirm the topological nature of the state. We find a quantized Hall conductivity of $\nu = 1/2$, the characteristic structure in the entanglement spectrum, the static

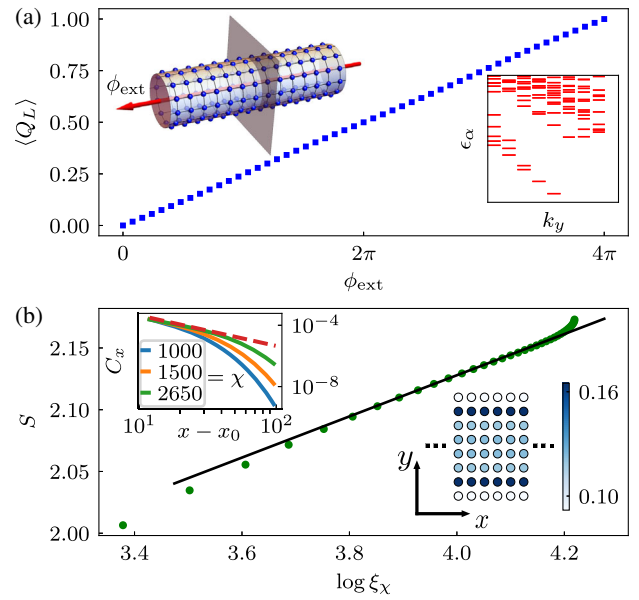


FIG. 2. Static properties of the bosonic $\nu = 1/2$ fractional Chern insulator. Panel (a) shows the pumping of a charge per two flux periods as expected for a $\nu = 1/2$ FCI state. The inset shows the entanglement spectrum of the zero charge sector. The low lying states satisfy the expected conformal field theory (CFT) counting $\{1, 1, 2, 3, 5, \dots\}$ (see also Ref. [40]). All data in (a) are calculated in an infinitely long cylinder with $L_y = 8$. Panel (b) shows the scaling of the entanglement entropy S as a function of the correlation length ξ_x for an infinite strip. The slope of $c/6$ determines the central charge of the edge theory $c = 1$. The lower right inset displays the real space charge density of a strip configuration, which is infinite in the x direction and finite in the y direction with $L_y = 8$. The upper left inset shows the ground-state correlation function $C_x = \langle a_x a_{x_0}^\dagger \rangle$ on the edge versus $x - x_0$ of an infinite strip with $L_y = 10$. The dashed line $\propto (x - x_0)^{-2}$ follows the Luttinger liquid theory prediction.

correlation function on the edge that approaches the prediction of Luttinger liquid theory with increasing bond dimension (χ), and a central charge of $c = 1$ for the edge theory through a finite entanglement scaling [47,48] when considering an infinite strip geometry. The latter quantity shows that the DMRG simulations on the infinite strip reproduce the expected critical behavior at the edge and that edge overlap is negligible for our choices of $L_y \geq 8$ [46,54].

Evolution of an added particle at the edge.—Having established the presence of the many-body FCI state at $1/8$ filling, we will now focus on the dynamical response. The results are shown in Fig. 1 and reveal characteristic differences between the single-particle and FCI case. We first investigate the single-particle case and consider the system on a strip geometry with open (periodic) boundary conditions along y (x). A particle is created at the edge of an empty lattice by acting on it with an a^\dagger operator and the resulting state is then evolved in time. Figure 1(a) shows the time evolution of the particle density on the edge which

exhibits no chirality; this can be understood by the following reasoning. The single-particle spectrum of the model [shown in the inset of Fig. 1(c)] possesses two dispersing midgap modes at different energies of opposite chiralities. These connect the central band ($C = -2$) to the top and bottom bands ($C = 1$) and *both* modes are exponentially localized at the edge of the finite strip. When creating a single particle at one edge, the state has overlap with both edge modes since both have support on the edge where the particle is created leading to the symmetric dispersion of the particle density. To verify the above interpretation, we compute the spectral function $A(k_x, \omega)$ as the Fourier transform in space and time of the dynamical correlation function $C_x(t) = \langle a_x(t) a_{x_0}^\dagger(t_0) \rangle$ for momentum k_x along the edge at frequency ω shown in Fig. 1(c). When compared to the energy spectrum of H [Fig. 1(c), inset], the spectral function highlights the fact that both midgap chiral states have overlap with the created particle, explaining the achiral behavior observed when simulating the time evolution.

For the interacting case, we consider an infinite strip geometry at $\nu = 1/2$ filling of the lowest band to prepare the system in an FCI ground state $|\Psi_{\text{strip}}^{\text{FCI}}\rangle$ [see lower right inset of Fig. 2(b)]. We again create a particle at the edge to obtain the state $|\Psi_i\rangle = a_i^\dagger |\Psi_{\text{strip}}^{\text{FCI}}\rangle$. We then simulate the time evolution of $|\Psi_i\rangle$ under the Hamiltonian H using a matrix-product operator based time evolution method [40,49–51]. Unlike in the free particle case, the propagation of the density is chiral [Fig. 1(b)] consistent with the single chiral branch in the spectral function [Fig. 1(d)]. In the FCI state, the emergent chirality is protected by the topology of the many-body wave function in the bulk and thus it is more robust than the single-particle case.

Trapping potential and dynamics.—With the insight gained previously it is possible to devise a protocol closer to what is experimentally realizable. In cold atomic systems, lasers are used to control the local density of particles, making it possible to create a local trapping potential of varying strength of the form [55,56]

$$H_\mu = \mu a_i^\dagger a_i. \quad (2)$$

We again restrict $i \in \text{edge}$ and compare the response of the single-particle case and the hardcore boson $\nu = 1/2$ FCI state as a function of μ . Our results are shown in Fig. 3 where we plot the Fourier transform of the particle density evolution on the edge, i.e., $\int dx \int dt e^{-i(kx - \omega t)} a_x^\dagger(t) a_x(t)$ with x on the edge (see also Ref. [40]). For the single-particle scenario in Figs. 3(a) and 3(c), we fill the lowest energy state of Hamiltonian (1) with one particle in the presence of a finite μ and then time evolve the resulting state with a quenched Hamiltonian by abruptly switching off the local potential. As a function of the trapping potential, the Fourier transform shows a nonsymmetric

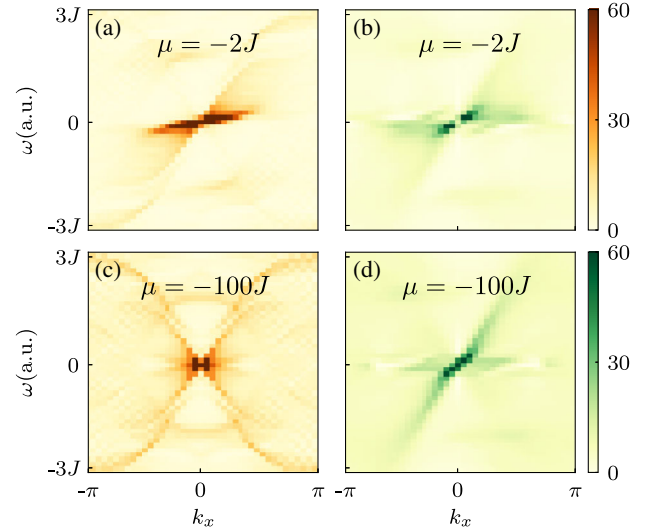


FIG. 3. Fourier transformation of the particle density evolution for a shallow ($\mu = -2 J$) and a deep trap ($\mu = -100 J$) localized at an edge site of the single-particle (a),(c) and FCI case (b),(d).

(symmetric) structure corresponding to a chiral (achiral) density evolution for a shallow (deep) trap [see Figs. 3(a) and 3(c)]. This difference originates from the fact that for a given μ , the evolving state can only explore a subset of the band structure. If μ is smaller than the gap between the lowest and central band, then the time evolution allows us to explore states only within one chiral edge state and thus exhibits chiral behavior. If μ is large compared to the total bandwidth, the initial state has overlap with the entire spectrum after switching off the potential. As discussed previously for Fig. 1(c), these states include two chiral modes of opposite chirality, and thus the chiral propagation disappears [Fig. 3(c)].

For the interacting case, we find the ground state for finite μ on an infinite strip at total filling $1/8$ with an extra particle using DMRG and, subsequently, let the state evolve under the quenched ($\mu = 0$) Hamiltonian. The $\nu = 1/2$ FCI state is a topologically ordered many-body state, and thus the single-particle band structure arguments do not apply. The evolution stays chiral for arbitrary trapping potential strength, as we observe in Figs. 3(b) and 3(d). In this case, the many-body state dictates the excitations at the edge which prove to be chiral in one direction. Taken together, the chiral evolution and the insensitivity to the trapping potential can be probed as an experimental signature of the $\nu = 1/2$ FCI state in this model, and is therefore one of the main results of this Letter.

In order to quantify the dependence of the chirality on the value of μ , we define the imbalance $\mathcal{I} = N_R - N_L$ of the total particle number on the edge to the left and right of site i during the time evolution in Figs. 4(a) and 4(b). The single-particle case is shown in Fig. 4(a) and the imbalance decreases with increasing the absolute value of μ consistent with the explanation above. For a very deep trap, the

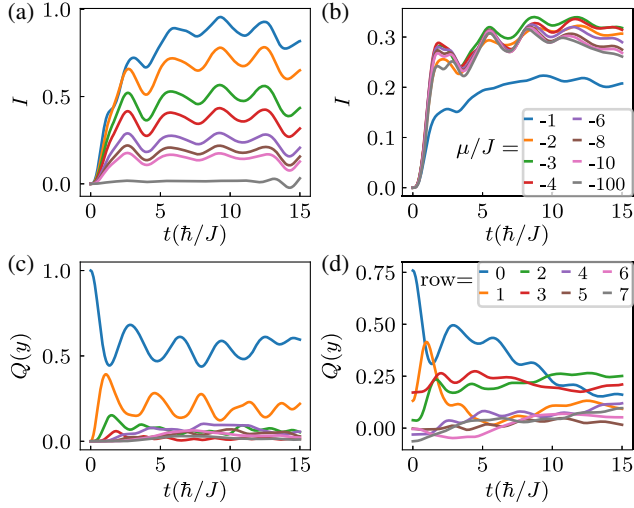


FIG. 4. The time evolution of the imbalance $\mathcal{I} = N_R - N_L$ between the total particle density on the right and left part of site i for the single-particle (a) and FCI (b) case for different values of the perturbation μ in units of the hopping J . For single particle (FCI) case the imbalance decreases (saturates) with increasing perturbation strength. Panels (c) and (d) show the total density per row as a function of time for the single-particle and the interacting scenario, respectively, for $\mu = -100$ J, showing a sizable leakage of particle density into the bulk. The legend indicates the row number in the y direction in the geometry of the inset of Fig. 2(b).

difference is almost zero, which denotes achiral behavior as expected. In contrast, the chiral behavior of the interacting topologically ordered state persists even for a very deep trap as shown in Fig. 4(b).

Towards a chiral Luttinger liquid description.—It is tempting to connect our previous analysis with the chiral Luttinger liquid of quantum Hall edge states [52]. For a Laughlin state at a filling $\nu = 1/m$, this description predicts that the spectral function and the density of states behave as [40,52]

$$A(k, \omega) \propto (\omega + vk)^{m-1} \delta(\omega - vk), \quad N(\omega) \propto \omega^{m-1}, \quad (3)$$

where v is the velocity of the edge state. A direct measurement of $A(k, \omega)$ or $N(\omega) = \int_k dk A(k, \omega)$ could be used to extract m , which would be solid evidence for the presence of the FCI state in experiment. Such analytical spectral function could be, in principle, compared directly to our numerical spectral function in Fig. 1(d). However, this exercise reveals two potential problems that experiments may face to extract m . First, the main differences between a trivial edge state and a chiral Luttinger liquid will be most drastic at longer times, or smaller ω . This region is, however, the most elusive numerically, due to entanglement growth, and experimentally, due to heating and particle loss. Second, particles created at the edge have a finite overlap with bulk states as the correlation length is finite [40]. Consequently, the particle will diffuse into the bulk at

longer times, making it difficult to resolve the low-energy (long time) behavior of the edge. We have numerically observed that a sizable part of the edge density is lost into the bulk. Our results are shown in Figs. 4(c) and 4(d) where we plot the average density per row for the free and interacting cases respectively when a particle is added at the edge (row $y = 0$). In both cases, we find that there is a leakage of density to the bulk, and the physical edge (i.e., the first row of sites) does not behave as an isolated liquid. In the single-particle case of Fig. 4(c), the particle density stabilizes after an initial drop, features that may be explained by the high overlap of the initial state with the exponentially localized edge eigenstates of the spectrum. The interacting case in Fig. 4(d) suffers from a more severe particle loss to the bulk of the system. We have attempted several protocols to decrease such a leakage. First, by increasing the width of the strip $L_y = 4, 8, 12$ we find no appreciable change in the density loss. This is consistent with the fact that for any finite width, the interactions between the two edge states are marginal for $\nu = 1/2$ [52]. Second, we have tried to confine the chiral edge modes with an additional negative chemical potential localized at the edge. We observed that although it reduces the leakage at long times, sufficient density is lost at short times to prevent a comparison with Eq. (3). Third, we find that the leakage is reduced by choosing $J_y/J_x < 1$. By studying the static properties as a function of J_y , we have checked that the FCI phase with $\nu = 1/2$ is stable up to strong anisotropies [31,34]. The smaller leakage as J_y decreases indicates that the correlation between the edge state and the bulk states in the y direction is the main source for particle loss.

Conclusions.—In this Letter, we have studied the dynamical properties of a bosonic fractional Chern insulator edge under local perturbations using the infinite density matrix renormalization group. We have dynamically established the chirality of the $\nu = 1/2$ bosonic FCI state emergent in the Harper-Hofstadter model at $1/8$ total filling, a relevant example for current cold atom experiments. We found that in the fractional Chern insulating phase a generic edge perturbation in this model propagates chirally, while the chirality in the single-particle case is only visible for weak perturbations, up to the order of the gap between the lowest and central band. This distinction can be carried over to Chern insulating models which host chiral edge modes with opposite chirality coexisting at a given edge, a common instance for multiband models, such as the Harper-Hofstadter model. In contrast, two band Chern insulator models, such as the Haldane model [12] realized experimentally [13] fall outside this category, and our approach is, in principle, not sufficient to distinguish the CI from the FCI state. However, in these models, if μ is larger than the single particle band gap, bulk excitations will be created, which will introduce larger noise to the chiral signal [57] than in their FCI counterparts, where the gap is set by the strong interaction energy scale. Our

simulations show that a particle created at the physical edge (i.e., first row of sites) has a finite overlap with bulk states and thus there is inevitable a density leakage, preventing a naive chiral Luttinger theory interpretation of the dynamics on the time scales considered.

Recently, a related example of the interplay between interactions and topology causing chiral dynamics was experimentally observed on a ladder system underlining the relevance of our results to ongoing experiments [7]. This experiment employed a boxlike confining potential that brings in line with our numerical simulations and which circumvents the effects of harmonic confinement [58,59]. A different realistic alternative is the engineering of sharp interfaces [60].

Our work highlights that in realistic experimental setups a richer dynamical behavior beyond a naive 1D Luttinger liquid behavior should be expected in fractional Chern insulators. It is triggered by an unforeseen density leakage from the first row of sites and the insensibility to the energy scales set by a perturbation localized to the edge, emphasizing the need for further studies of dynamics of fractional Chern insulators.

We thank N. Goldman, F. Grusdt, M. Kolodrubetz, N. Regnault, and R. Vasseur for fruitful discussions and suggestions. A. G. G. was supported by the Marie Curie Programme under EC Grant agreement No. 653846. J. M. acknowledges funding by TIMES at Lawrence Berkeley National Laboratory supported by the U.S. Department of Energy, Office of Basic Energy Sciences, Division of Materials Sciences and Engineering, under Contract No. DE-AC02-76SF00515 and through DFG research fellowship MO 3278/1-1. F. P. acknowledges support from DFG through Research Unit FOR 1807 with Grant No. PO 1370/2-1 and from the Nanosystems Initiative Munich (NIM) by the German Excellence Initiative, and the European Research Council (ERC) under the European Union's Horizon 2020 research and innovation program (Grant agreement No. 771537).

[1] A. Polkovnikov, K. Sengupta, A. Silva, and M. Vengalattore, Colloquium: Nonequilibrium dynamics of closed interacting quantum systems, *Rev. Mod. Phys.* **83**, 863 (2011).
 [2] J. Eisert, M. Friesdorf, and C. Gogolin, Quantum many-body systems out of equilibrium, *Nat. Phys.* **11**, 124 (2015).
 [3] C. Becke *et al.*, Ultracold quantum gases in triangular optical lattices, *New J. Phys.* **12**, 065025 (2010).
 [4] S. Trotzky, Y.-A. Chen, A. Flesch, I. P. McCulloch, U. Schollwöck, J. Eisert, and I. Bloch, Probing the relaxation towards equilibrium in an isolated strongly correlated one-dimensional Bose gas, *Nat. Phys.* **8**, 325 (2012).
 [5] M. Schreiber, S. S. Hodgman, P. Bordia, H. P. Lüschen, M. H. Fischer, R. Vosk, E. Altman, U. Schneider, and I. Bloch, Observation of many-body localization of interacting fermions in a quasirandom optical lattice, *Science* **349**, 842 (2015).

[6] J.-y. Choi, S. Hild, J. Zeiher, P. Schauß, A. Rubio-Abadal, T. Yefsah, V. Khemani, D. A. Huse, I. Bloch, and C. Gross, Exploring the many-body localization transition in two dimensions, *Science* **352**, 1547 (2016).
 [7] M. E. Tai, A. Lukin, M. Rispoli, R. Schittko, T. Menke, D. Borgnia, P. M. Preiss, F. Grusdt, A. M. Kaufman, and M. Greiner, Microscopy of the interacting Harper–Hofstadter model in the two-body limit, *Nature (London)* **546**, 519 (2017).
 [8] P. G. Harper, Single Band Motion of Conduction Electrons in a Uniform Magnetic Field, *Proc. Phys. Soc. A* **68**, 874 (1955).
 [9] D. R. Hofstadter, Energy levels and wave functions of Bloch electrons in rational and irrational magnetic fields, *Phys. Rev. B* **14**, 2239 (1976).
 [10] M. Aidelsburger, M. Atala, M. Lohse, J. T. Barreiro, B. Paredes, and I. Bloch, Realization of the Hofstadter Hamiltonian with Ultracold Atoms in Optical Lattices, *Phys. Rev. Lett.* **111**, 185301 (2013).
 [11] H. Miyake, G. A. Siviloglou, C. J. Kennedy, W. C. Burton, and W. Ketterle, Realizing the Harper Hamiltonian with Laser-Assisted Tunneling in Optical Lattices, *Phys. Rev. Lett.* **111**, 185302 (2013).
 [12] F. D. M. Haldane, Model for a Quantum Hall Effect without Landau Levels: Condensed-Matter Realization of the Parity Anomaly, *Phys. Rev. Lett.* **61**, 2015 (1988).
 [13] G. Jotzu, M. Messer, R. Desbuquois, M. Lebrat, T. Uehlinger, D. Greif, and T. Esslinger, Experimental realization of the topological Haldane model with ultracold fermions, *Nature (London)* **515**, 237 (2014).
 [14] D. Jaksch and P. Zoller, Creation of effective magnetic fields in optical lattices: the Hofstadter butterfly for cold neutral atoms, *New J. Phys.* **5**, 56 (2003).
 [15] S. Rahav, I. Gilary, and S. Fishman, Effective Hamiltonians for periodically driven systems, *Phys. Rev. A* **68**, 013820 (2003).
 [16] J. Dalibard, F. Gerbier, G. Juzeliūnas, and P. Öhberg, Colloquium: Artificial gauge potentials for neutral atoms, *Rev. Mod. Phys.* **83**, 1523 (2011).
 [17] N. Goldman, J. C. Budich, and P. Zoller, Topological quantum matter with ultracold gases in optical lattices, *Nat. Phys.* **12**, 639 (2016).
 [18] A. Eckardt, Colloquium: Atomic quantum gases in periodically driven optical lattices, *Rev. Mod. Phys.* **89**, 011004 (2017).
 [19] A. G. Grushin, A. Gómez-León, and T. Neupert, Floquet fractional Chern insulators, *Phys. Rev. Lett.* **112**, 156801 (2014).
 [20] E. Anisimovas, G. Žlabys, B. M. Anderson, G. Juzeliūnas, and A. Eckardt, Role of real-space micromotion for bosonic and fermionic Floquet fractional Chern insulators, *Phys. Rev. B* **91**, 245135 (2015).
 [21] M. Račiūnas, G. Žlabys, A. Eckardt, and E. Anisimovas, Modified interactions in a Floquet topological system on a square lattice and their impact on a bosonic fractional Chern insulator state, *Phys. Rev. A* **93**, 043618 (2016).
 [22] E. J. Bergholtz and Z. Liu, Topological flat band models and fractional Chern insulators, *Int. J. Mod. Phys. B* **27**, 1330017 (2013).
 [23] T. Neupert, C. Chamon, T. Iadecola, L. H. Santos, and C. Mudry, Fractional (Chern and topological) insulators, *Phys. Scr.* **2015**, 014005 (2015).

- [24] T. Neupert, L. Santos, C. Chamon, and C. Mudry, Fractional Quantum Hall States at Zero Magnetic Field, *Phys. Rev. Lett.* **106**, 236804 (2011).
- [25] E. Tang, J.-W. Mei, and X.-G. Wen, High Temperature Fractional Quantum Hall States, *Phys. Rev. Lett.* **106**, 236802 (2011).
- [26] K. Sun, Z. Gu, H. Katsura, and S. D. Sarma, Nearly flatbands with nontrivial topology, *Phys. Rev. Lett.* **106**, 236803 (2011).
- [27] N. Regnault and B. A. Bernevig, Fractional Chern Insulator, *Phys. Rev. X* **1**, 021014 (2011).
- [28] Y.-L. Wu, B. A. Bernevig, and N. Regnault, Zoology of fractional Chern insulators, *Phys. Rev. B* **85**, 075116 (2012).
- [29] M. Hafezi, A. S. Sørensen, E. Demler, and M. D. Lukin, Fractional quantum Hall effect in optical lattices, *Phys. Rev. A* **76**, 023613 (2007).
- [30] G. Möller and N. R. Cooper, Composite Fermion Theory for Bosonic Quantum Hall States on Lattices, *Phys. Rev. Lett.* **103**, 105303 (2009).
- [31] Y.-C. He, F. Grusdt, A. Kaufman, M. Greiner, and A. Vishwanath, Realizing and Adiabatically Preparing Bosonic Integer and Fractional Quantum Hall states in Optical Lattices, *Phys. Rev. B* **96**, 201103 (2017).
- [32] M. Gerster, M. Rizzi, P. Silvi, M. Dalmonte, and S. Montangero, Fractional quantum Hall effect in the interacting Hofstadter model via tensor networks, *Phys. Rev. B* **96**, 195123 (2017).
- [33] J. Motruk and F. Pollmann, Phase transitions and adiabatic preparation of a fractional Chern insulator in a bosonic cold atom model, *Phys. Rev. B* **96**, 165107 (2017).
- [34] D. Hügél, H. U. R. Strand, P. Werner, and L. Pollet, Anisotropic Harper-Hofstadter-Mott model: Competition between condensation and magnetic fields, *Phys. Rev. B* **96**, 054431 (2017).
- [35] A. S. Sørensen, E. Demler, and M. D. Lukin, Fractional Quantum Hall States of Atoms in Optical Lattices, *Phys. Rev. Lett.* **94**, 086803 (2005).
- [36] I. B. Spielman, Detection of topological matter with quantum gases, *Ann. Phys. (Amsterdam)* **525**, 797 (2013).
- [37] N. Goldman, J. Dalibard, A. Dauphin, F. Gerbier, M. Lewenstein, P. Zoller, and I. B. Spielman, Direct imaging of topological edge states in cold-atom systems, *Proc. Natl. Acad. Sci. U.S.A.* **110**, 6736 (2013).
- [38] N. Goldman, J. Beugnon, and F. Gerbier, Detecting Chiral Edge States in the Hofstadter Optical Lattice, *Phys. Rev. Lett.* **108**, 255303 (2012).
- [39] L. Cincio and G. Vidal, Characterizing topological order by studying the ground states on an infinite cylinder, *Phys. Rev. Lett.* **110**, 067208 (2013).
- [40] See Supplemental Material at <http://link.aps.org/supplemental/10.1103/PhysRevLett.121.086401> for details on the model, the computation of the static properties, a summary of chiral Luttinger liquid theory, the real space time evolution of the edge state density distribution, and further discussion on the density leakage, which includes Refs. [41–53].
- [41] I. P. McCulloch, Infinite size density matrix renormalization group, revisited, [arXiv:0804.2509](https://arxiv.org/abs/0804.2509).
- [42] J. A. Kjäll, M. P. Zaletel, R. S. K. Mong, J. H. Bardarson, and F. Pollmann, Phase diagram of the anisotropic spin-2 XXZ model: Infinite-system density matrix renormalization group study, *Phys. Rev. B* **87**, 235106 (2013).
- [43] R. B. Laughlin, Quantized Hall conductivity in two dimensions, *Phys. Rev. B* **23**, 5632 (1981).
- [44] M. P. Zaletel, R. S. K. Mong, and F. Pollmann, Flux insertion, entanglement, and quantized responses, *J. Stat. Mech.* **10** (2014) P10007.
- [45] A. G. Grushin, J. Motruk, M. P. Zaletel, and F. Pollmann, Characterization and stability of a fermionic $\nu = 1/3$ fractional Chern insulator, *Phys. Rev. B* **91**, 035136 (2015).
- [46] H. Li and F. D. M. Haldane, Entanglement Spectrum as a Generalization of Entanglement Entropy: Identification of Topological Order in Non-Abelian Fractional Quantum Hall Effect States, *Phys. Rev. Lett.* **101**, 010504 (2008).
- [47] L. Tagliacozzo, T. R. de Oliveira, S. Iblisdir, and J. I. Latorre, Scaling of entanglement support for matrix product states, *Phys. Rev. B* **78**, 024410 (2008).
- [48] F. Pollmann, S. Mukerjee, A. M. Turner, and J. E. Moore, Theory of Finite-Entanglement Scaling at One-Dimensional Quantum Critical Points, *Phys. Rev. Lett.* **102**, 255701 (2009).
- [49] J. A. Kjäll, F. Pollmann, and J. E. Moore, Bound states and E_8 symmetry effects in perturbed quantum Ising chains, *Phys. Rev. B* **83**, 020407 (2011).
- [50] M. P. Zaletel, R. S. K. Mong, C. Karrasch, J. E. Moore, and F. Pollmann, Time-evolving a matrix product state with long-ranged interactions, *Phys. Rev. B* **91**, 165112 (2015).
- [51] M. Gohlke, R. Verresen, R. Moessner, and F. Pollmann, Dynamics of the Kitaev-Heisenberg Model, *Phys. Rev. Lett.* **119**, 157203 (2017).
- [52] X. G. Wen, Chiral Luttinger liquid and the edge excitations in the fractional quantum Hall states, *Phys. Rev. B* **41**, 12838 (1990).
- [53] M. Aidelsburger, M. Lohse, C. Schweizer, M. Atala, J. T. Barreiro, S. Nascimbene, N. R. Cooper, I. Bloch, and N. Goldman, Measuring the Chern number of Hofstadter bands with ultracold bosonic atoms, *Nat. Phys.* **11**, 162 (2014).
- [54] P. Calabrese and J. Cardy, Entanglement entropy and quantum field theory, *J. Stat. Mech.* **06** (2004) P06002.
- [55] W. S. Bakr, J. I. Gillen, A. Peng, S. Fölling, and M. Greiner, A quantum gas microscope for detecting single atoms in a Hubbard-regime optical lattice, *Nature (London)* **462**, 74 (2009).
- [56] T. A. Hilker, G. Salomon, F. Grusdt, A. Omran, M. Boll, E. Demler, I. Bloch, and C. Gross, Revealing hidden anti-ferromagnetic correlations in doped Hubbard chains via string correlators, *Science* **357**, 484 (2017).
- [57] A. G. Grushin, S. Roy, and M. Haque, Response of fermions in Chern bands to spatially local quenches, *J. Stat. Mech.* **08** (2016) 083103.
- [58] M. Buchhold, D. Cocks, and W. Hofstetter, Effects of smooth boundaries on topological edge modes in optical lattices, *Phys. Rev. A* **85**, 063614 (2012).
- [59] N. Goldman, J. Beugnon, and F. Gerbier, Identifying topological edge states in 2D optical lattices using light scattering, *Eur. Phys. J. Spec. Top.* **217**, 135 (2013).
- [60] N. Goldman, G. Jotzu, M. Messer, F. Görg, R. Desbuquois, and T. Esslinger, Creating topological interfaces and detecting chiral edge modes in a two-dimensional optical lattice, *Phys. Rev. A* **94**, 043611 (2016).